Reaction of H_2 with mitochondria-relevant metabolites using a multifunctional molecular catalyst

Authors: Sota Nimura,[2] Shota Yoshioka,[2] Masayuki Naruto,[2] and Susumu Saito*[1,2]

Affiliations:

[1]Research Center for Materials Science, Nagoya University, Chikusa, Nagoya 464-8602, Japan.

[2]Graduate School of Science, Nagoya University, Chikusa, Nagoya 464-8602, Japan.

*Correspondence to: saito.susumu@f.mbox.nagoya-u.ac.jp.

Abstract: The Krebs cycle is the fuel/energy source for cellular activity, and therefore of paramount importance for oxygen-based life. The cycle occurs in the mitochondrial matrix, where it produces and transfers electrons to generate energy-rich NADH and $FADH_2$, as well as C_4-, C_5-, and C_6-polycarboxylic acids as energy-poor metabolites. These metabolites are bio-renewable resources that represent potential sustainable carbon feedstocks, provided that carbon–hydrogen bonds are restored to these molecules. In the present study, these polycarboxylic acids and other mitochondria-relevant metabolites are dehydrated and reduced to diols or triols upon reaction with H_2, catalyzed by sterically confined iridium-bipyridyl complexes. The investigation of these single-metal-site catalysts provides valuable molecular insights into the development of molecular technologies for the reduction and dehydration of highly functionalized carbon resources.

One Sentence Summary: (PNNP)Iridium complexes remove H_2O from and deliver electrons and hydrogen atoms to Krebs-cycle metabolites to make them energy-rich.

Main Text:

The recent depletion of fossil fuel resources has impelled industrial and academic researchers to search for alternative carbon-based energy sources. Considerable effort has been invested in biotechnology and sustainable/green technologies to develop a chemical industry in which renewable energy resources complement dwindling fossil fuel sources for the new millennium. A round-table discussion of the US Department of Energy (DOE) identified the top 30 value-added chemicals derived from biomass, which included various (poly)carboxylic acids and polyols (*1*). These chemicals exist in high oxidation and/or highly oxygenated states, and thus, current state-of-the-art oxidation catalysts must be substantially modified in order to achieve the reduction and dehydration of such bio-renewable resources (*2,3*).

The top 30 value-added chemicals in the aforementioned list, which is continually re-evaluated, were further narrowed to a top 12 list, in which the highest value-added carboxylic acid (CA) is succinic acid (SucA) (*4,5*). In particular, the eight-hydrogen-atom (or 8e)-reduced, doubly dehydrated form of SucA, 1,4-butanediol (1,4-BDO), is a highly versatile synthetic intermediate. 1,4-BDO is an important commodity chemical used to manufacture over 2.5 million tons of valuable polymers per year, including poly(butylene) terephthalate and poly(urethane)s (*6*). Yet, reports dealing with the selective reduction of SucA to 1,4-BDO using molecular catalysis are scarce, particularly those reporting systematic trial-and-error investigations (*5,7,8*). Various patents and scientific articles on the topic of heterogeneous catalysts for the hydrogenation of SucA have reported that numerous reaction parameters

influence the product distribution (*5,9*); thus, the development of more sophisticated catalysts is required to control the product yields. In addition, identification of the most crucial catalytic site at the molecular level is difficult in heterogenous catalysts, as their heterogeneous surfaces contain many different catalytic islands.

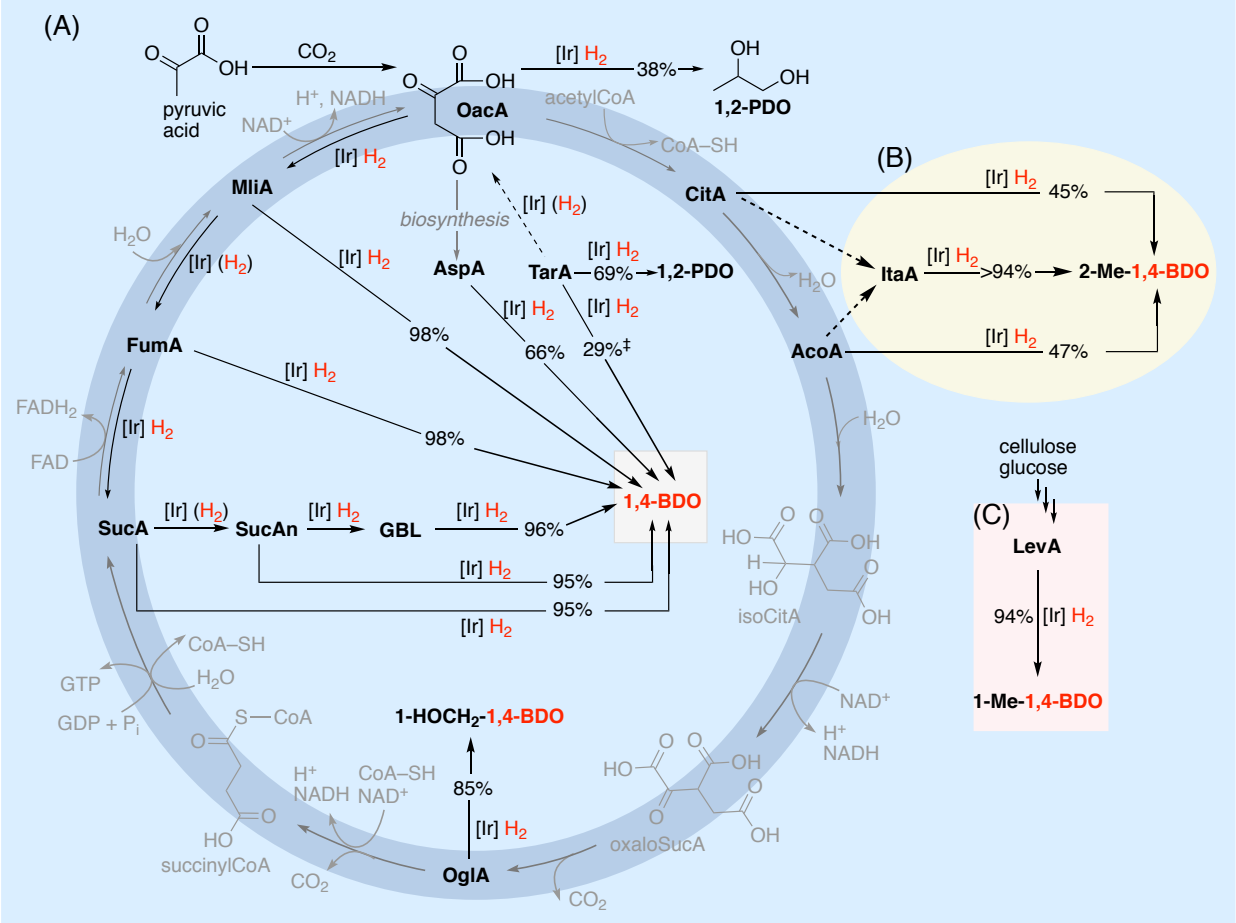

Fig. 1. Redrawing the map for the chemical transformation of Krebs-cycle-relevant metabolites. (A) Single-[Ir]-site-catalyzed hydrogenation and dehydration reactions in this work (black arrows and red text), and the original Krebs cycle (blue ring and gray text/arrows). Dotted arrows are proposed partial pathways in the hydrogenation of each substrate with Ir-**a**. ‡1,2-PDO (36%) was also obtained. (B) Hydrogenation of cytoplasm metabolites (pale green ellipse). (C) Hydrogenation of the sugar-derived artificial feedstock LevA. For definitions of abbreviations and acronyms, see Fig. 2a. IsoCitA, oxaloSucA, and succinylCoA are not commercially available.

In addition to SucA, significant attention should be paid to the reduction and dehydration of more highly functionalized C_4-, C_5-, and C_6-polycarboxylic acids (PCAs, including dicarboxylic acids (DCAs) and tricarboxylic acids (TCAs)), such as fumaric acid (FumA) (*10*), malic acid (MliA) (*11*), oxaloacetic acid (OacA) (*12*), 2-oxoglutaric acid (OglA) (*13*), aconitic acid (AcoA) (*14*), and citric acid (CitA) (*15*), which are potential carbon feedstocks produced as metabolites in the Krebs cycle (*16*) (also known as the tricaboxylic acid (TCA) cycle or citric acid cycle)

(Figs. 1a and 2a), which operates in the mitochondrial matrix in the cells of most plants, animals, fungi, and many bacteria. Further biotechnological modification of this energy-yielding metabolic pathway could enable the scalable production of C_4-, C_5-, and C_6-PCAs, which can be expected to be upgraded subsequently using catalysts that effectively reduce and dehydrate these compounds (the goal of this research). The Krebs cycle is mainly controlled by oxidation and hydration (with decarboxylation) reactions of various enzymes. The hydrogen (electron)-trapping cofactors NAD^+ and FAD^+ are involved in controlling the product distribution across different C_4-, C_5-, and C_6-PCAs. If an artificial catalyst was able to reverse the natural Krebs cycle (written formally in a clockwise fashion in Fig. 1a) by promoting the usually unfavorable reduction (hydrogenation) and dehydration [hydrogenolysis/hydrodeoxygenation (HDO) (*17,18*): $R_{3-n}CH_nOH + 2\ H \rightarrow R_{3-n}CH_{n+1} + H_2O$ (n = 0–3)] reactions in an anti-clockwise fashion, diverse functionalized C_4-, C_5-, and C_6-metabolites could be transformed into a family of energy-rich polyols (1,4-BDO derivatives and C_3-diols) without recruiting natural enzymes.

In this context, the development of novel, robust, and unidirectional catalysts, i.e., catalysts that promote hydrogenations and dehydrations while they suppress the reverse processes, represents a great challenge, since the highly oxygenated or nitrogenated substrates abundant in nature can easily poison catalytically active sites via substrate/product inhibition, and the reverse dehydrogenation reaction sometimes occurs, particularly at high temperature. Moreover, the design of a molecular catalytic active site and clarification of the complex multistep reduction mechanisms such as the 10-electron (10e) reduction of FumA to 1,4-BDO would be highly desirable; unfortunately, however, systematic studies to establish a molecular rationale and molecularly predictable approaches to obtain high productivity and selectivity in divergent reduction/dehydration reactions of PCAs all the way to different polyol products remain elusive.

As part of our ongoing interest in developing new molecular technologies for the catalytic reduction and/or dehydration of organic compounds in high oxidation states (*19*), peptides and plastics (*20, 21*), monocarboxylic acids (MCA) including fatty acids and α-amino acids (*22, 23, 24,25*), and bio-alcohols (*26*), we introduce here the coordinatively saturated (PNNP)iridium (Ir) complex Ir-**a** (Fig. 2). Ir-**a** is a novel, versatile, and robust precatalyst, whose multifunctional, sterically confined Ir-bipyridyl (bpy) framework can promote various dehydration and hydrogenation processes in a one-pot fashion; the apparent cleavage of C–O and C–N σ bonds under concomitant decarboxylation to induce HDO and even hydrodeamination (HDA) reactions is followed by the hydrogenation of various C=C and C=O bonds of ketones, acid anhydrides, and esters, which affords C_3, C_4, and C_5 carbon feedstocks (Fig. 2a). The catalytic framework generated upon addition of n H_2 (n = 1–6) to Ir-**a** maintains its structural robustness, with no detachment of the ligand from the Ir center or C–P bond cleavage (*20*). Thus, the complex retains good catalytic activity even under strenuous conditions (hydrogen pressure (P_{H2}): 4–8 MPa; reaction temperature (T): 140–200 °C; reaction time (t): 18–120 h). The single catalytic active site of this bespoke Ir–bpy framework is sterically protected by four cyclohexyl (Cy) groups; the small size of the active pocket favors the selective uptake, coordination, and activation of H_2 (Fig. 2b, left). The confined environment of the single-metal-site also protects the catalyst from deactivation via bidentate coordination by the relatively large functional groups of the highly oxygenated and nitrogenated compounds, and even from monodentate coordination to the virtually coordinatively saturated Ir center.

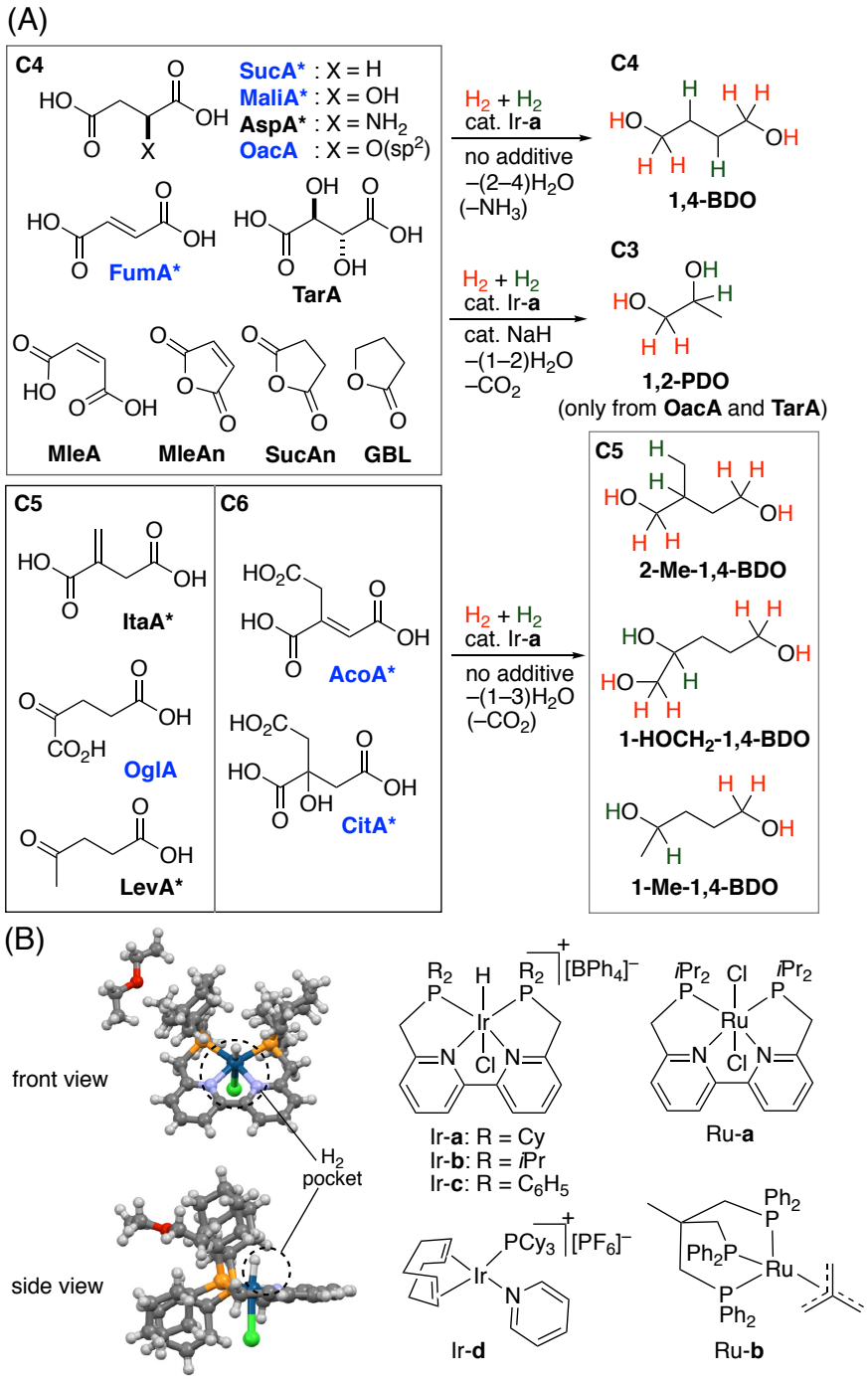

Fig. 2. Summary of this work. (A) Renewable carbon feedstocks that afford various 1,4-BDO derivatives and 1,2-PDO. Compound names in blue are Krebs cycle metabolites, while those marked with asterisks are possible feedstocks listed as top 30 value-added chemicals in the initial DOE/NREL report in 2004 (*1*). (B) Single-crystal x-ray diffraction structure of Ir-**a** (left; Et_2O included). Color key: Ir (blue), N (purple), P (orange), Cl (green), O (red), H (white). See also ESI, Fig. S1. $[BPh_4]^-$ is omitted for clarity. Ir- and Ru complexes for hydrogenation tested in this work (right).

Reaction of H_2 with C_4-DCAs and their anhydrides. We have recently reported that the (PNNP)ruthenium (Ru) complex Ru-**a** (Fig. 2b, right) serves as a molecular precatalyst for the hydrogenation of unactivated amides, including polymer nylons (*20*). However, Ru-**a** (1 mol %) was ineffective for the hydrogenation of SucA to 1,4-BDO (Fig. 3a, entry 1) under the reaction conditions used for amide hydrogenation (NaH (10 mol %); P_{H2} = 6 MPa; T = 180 °C), and only γ-butyrolactone (GBL) was produced in 21% yield. We then screened different metal centers with different tetradentate PNNP ligands in the presence of a catalytic amount of NaH for the hydrogenation of SucA, and found that iridium (Ir) complex Ir-**a** (1 mol %; $[\text{Ir-}\mathbf{a}]_0$ = 5.0 mM; $[\text{SucA}]_0$ = 0.50 M; [NaH] = 6 mol %; $[\text{Ir-}\mathbf{a}]_0$:$[\text{NaH}]_0$ = 1:6) was the most effective to furnish 1,4-BDO in 95% yield (GBL: 5%). The state-of-the-art Ir-complex Ir-**d** (Crabtree complex (*27*)) was also tested (Fig. 3a, entry 5), albeit that it showed, similar to the water-soluble Vaska complex, merely scant activity, producing only GBL (*5*).

The intended role of NaH was to remove a methylene (CH_2PCy_2) hydrogen atom from Ir-**a** to promote the dearomatization of a bipyridyl (bpy) fragment (*19, 20, 28, 29*). This step may be followed by the full hydrogenation of the bpy framework under strenuous conditions; Ru-**a** undergoes such deprotonation and hydrogenation in the presence of NaH (*20, 21*). However, after numerous control experiments for the hydrogenation of SucA ($[\text{SucA}]_0$ = 0.22 M) with Ir-**a** (1.5 mol %), we found that a comparable hydrogenation of SucA occurs even *without NaH* in toluene, which generates 1,4-BDO in 86±8% yield (average of six runs) under otherwise identical conditions (Fig. 3b, entry 1; ESI, Table S1). Ir-**a** derivatives Ir-**b** and Ir-**c**, which bear similar PNNP ligands with different steric demands, showed comparable or lower catalytic activity (Fig. 3b, entries 2 and 3). The groups of Leitner and Klankermayer as well as that of Frediani have previously reported that Ru–Triphos ($(Ph_2PCH_2)_3CMe$) catalyzes the hydrogenation of SucA under harsh conditions (*7, 8*) (P_{H2} = ca. 5–8 MPa; T = 150–195 °C; t = 24–27 h). Therefore, we retested Ru-Triphos complex Ru-**b** (1.5 mol %) in both the presence and absence of NaH (Fig 3a, entries 2 and 3), and found that its catalytic activity (1,4-BDO: 83–90%; three independent runs) was comparable to that of Ir-**a** under identical reaction conditions (P_{H2} = 6 MPa; T = 180 °C, t = 18 h). Both the P_{H2} and T values are critical for the production of the desired product 1,4-BDO; GBL was formed exclusively in good to moderate yield at lower temperatures (79%; T = 160 °C; t = 36 h) or at lower P_{H2} (58%; 4 MPa; t = 18 h; $[\text{SucA}]_0$ = 0.50 M) (ESI, Table S2). GBL was hydrogenated almost quantitatively to 1,4-BDO by Ir-**a** (1.5 mol %) within 4 h at 180 °C or within 18 h at 160 °C, while the yield at 160 °C was marginal after 4 h (Fig. 3b, entry 13; ESI, Table S3). Capitalizing on the versatility of Ir-**a**, the dehydrogenated forms of SucA, i.e., FumA and its *Z*-isomer MleA, were also hydrogenated smoothly to give 1,4-BDO in near quantitative yield (Fig. 3b, entries 4 and 5). The anhydrides of SucA (SucAn) and MleA (MleAn) were also hydrogenated to exclusively produce 1,4-BDO (Fig. 3b, entries 11 and 12), although the hydrogenation of MleAn was somewhat sluggish (t = 18 h: 35%; t = 42 h: 88%; t = 66 h: 91%). All control experiments suggest that the hydrogenation of FumA to 1,4-BDO follows the pathway FumA→SucA→SucAn→GBL→1,4-BDO.

(A)

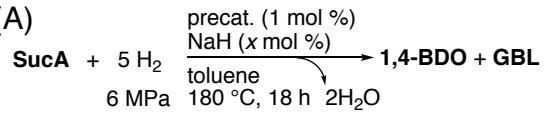

entry	precat.	NaH x (mol %)	**1,4-BDO** yield (%)[b]	**GBL** yield (%)[b]
1	Ru-**a**	10	nd[c]	21
2	Ru-**b**	6	75	3
3	Ru-**b**	0	90	3
4	Ir-**a**	6	95	5
5	Ir-**d**	6	nd	19

[a]Unless otherwise specified, the reactions were carried out using precat.:SucA:NaH = 1:100:0–10 mol % in toluene for 18 h, starting with P_{H2} = 6 MPa at 25 °C. [b] ^{1}H NMR (DMSO-d_6) based on internal standard. [c]Not detected by ^{1}H NMR.

(B)

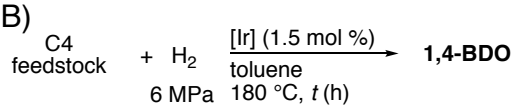

entry	C4 feedstock	t (h)	**1,4-BDO** yield (%)[b]	**GBL** yield (%)[b]
1	**SucA**	18, 42	86±8[h], 91	5±2[h], 2
2[c]	**SucA**	18	44	41
3[d]	**SucA**	18	81	2
4	**FumA**	18, 42	81, 98	3, 2
5	**MleA**	18, 42	80, 97	16, 3
6	**MliA**	42	98	2
7[e]	**AspA**	66	66	4
8	**TarA**	90	29(36)[g]	–[i]
9[f]	**TarA**	90	14(69)[g]	–[i]
10[f]	**OacA**	24	~1(38)[g]	–[i]
11	**MleAn**	18, 42, 66	35, 88, 91	28, 2, 3
12	**SucAn**	4, 8	7, 95	62, 2
13	**GBL**	4	96	–[i]

[a]Unless otherwise specified, the reactions were carried out using Ir-**a**:feedstock = 1.5:100 mol % in toluene, starting with P_{H2} = 6 MPa at 25 °C. [b] ^{1}H NMR yield (DMSO-d_6), based on internal standard. [c]Ir-**b**. [d]Ir-**c**. [e]Byproduct: 2-pyrrolidone (12%). [f]NaH (9 mol %) was used. [g]Yield of 1,2-PDO. [h]Average of 6 runs. [i]Not detected.

(C)

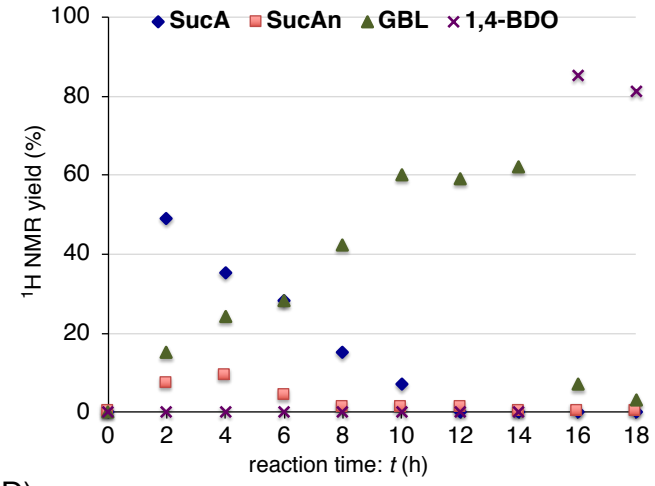

(D)

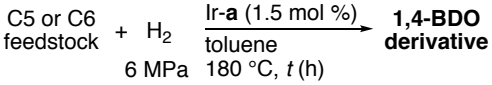

entry	C5 or C6 feedstock	t (h)	main product	**1,4-BDO deriv.** yield (%)[b]	**GBL deriv.** yield (%)[b]
1	**OglA**	72	**1-HOCH$_2$-1,4-BDO**	85(78)[c]	nd[d]
2	**AcoA**	120	**2-Me-1,4-BDO**	47(42)[c]	nd[d]
3	**CitA**	120	**2-Me-1,4-BDO**	45(32)[c]	nd[d]
4[e]	**ItaA**	72	**2-Me-1,4-BDO**	>94	<6[f]
5	**LevA**	18	**1-Me-1,4-BDO**	94	6

[a]Unless otherwise specified, the reactions were carried out using Ir-**a**:feedstock = 1.5:100 mol % in toluene, starting with P_{H2} = 6 MPa at 25 °C. [b] ^{1}H NMR yield (DMSO-d_6), based on internal standard. [c]Yield of the isolated, purified prodcut. [d]Not determined. [e]Using 1,4-dioxane instead of toluene. [f]2-Me- (<2%) and 3-Me-GBL (<2%).

(E)

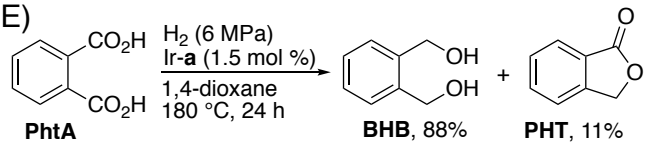

Fig. 3. Experimental results: Hydrogenation of various C$_4$-, C$_5$-, and C$_6$-PCA feedstocks and PhtA using Ir-a and other metal complexes. (A) Hydrogenation of SucA with different Ir- and Ru complexes. (B) Hydrogenation of C$_4$-feedstocks with Ir-**a**, Ir-**b,** and Ir-**c**. (C) Time-conversion (yield) plots of the hydrogenation of FumA with Ir-**a** (1.5 mol %) w/o NaH. (D) Hydrogenation of C$_5$ and C$_6$ feedstocks with Ir-**a**. (E) Hydrogenation of phthalic acid (PhtA) with Ir-**a**.

We then determined the time–conversion profile during the Ir-**a** (1.5 mol %)-promoted hydrogenation of FumA ([Ir-**a**]$_0$ = 7.5 mM; [FumA]$_0$ = 0.50 M; in toluene; P_{H2} = 6 MPa; T = 180 °C; t = 0–18 h) and plotted the changes in the product distribution as a function of time (Fig. 3c; ESI, Tables S4 and S5). FumA was rapidly hydrogenated to SucA (2e reduction: t < 1 h), which was consistently detected over the first 12 h of reaction. The conversion of SucA to GBL

was slow (t: 10–12 h), while the concentration of SucAn was negligible until t = 18 h, which suggests that SucAn, once formed, was rapidly hydrogenated to GBL (4e reduction), even in the presence of SucA, which provided slightly acidic conditions. Interestingly, the subsequent hydrogenation of GBL to 1,4-BDO (4e reduction) did not begin until SucA had completely disappeared (t = ~14 h). Upon complete consumption of SucA, the hydrogenation of GBL commenced suddenly, and was completed within 2 h. It can thus be concluded that the catalyst for the hydrogenation of GBL is resting in an inactive form under acidic conditions provided by the inherent acidity of SucA. Additional control experiments revealed that the hydrogenation of SucAn at 180 °C for 4 h resulted in the selective formation of GBL in 62% yield (1,4-BDO (7%) + oligomeric esters) (Fig 3b, entry 12). During the overall reaction to produce 1,4-BDO from FumA (FumA→SucA→SucAn→GBL→1,4-BDO), the slowest reaction step was the dehydrative cyclization of SucA to SucAn, which required ca. 12 h. A similar time profile of the product distribution was observed under the relatively basic conditions provided by the combined use of Ir-**a** and NaH (1.5:9 mol %) (ESI, Fig. S2), except that the complete conversion of SucA to SucAn was faster (ca. 10 h vs. 14 h w/o NaH (*vide supra*)) and the hydrogenation of GBL (+ oligomeric esters) to 1,4-BDO was slower (ca. 6 h vs. 2 h w/o NaH (*vide supra*)).

Reaction of H_2 with more functionalized C_4-DCAs. Subsequently, we investigated the hydrogenation of MliA, AspA, and TarA, i.e., functionalized C_4-DCAs that are structurally relevant to SucA. MliA is a Krebs cycle metabolite (*11, 16*); AspA is biosynthesized by the transamination of oxaloacetic acid (OacA: Krebs cycle metabolite) via enzymatic processes involving aspartase (*30*). Tartalic acid (TarA) can be produced from vitamin C (L-ascorbic acid; or from 5-oxo-D-gluconic acid) by scalable fermentation (*31*). Since Ru-**b** showed catalytic activity similar to that of Ir-**a** for the hydrogenation of SucA (*vide supra*), the hydrogenation of these C_4-DCAs using catalytic amounts of Ru-**b** was examined (P_{H2} = 6 MPa; T = 180 °C, t = 18–90 h) (ESI, Table S6). MliA was hydrogenated to 1,4-BDO; the yield of 1,4-BDO was found to be the same (70±1%) at t = 18 h and 42 h. This result suggests that the Ru-**b**-derived catalyst is relatively vulnerable and deactivated within 18 h, while the Ir-**a**-derived catalyst continues to show good activity thereafter (1,4-BDO: 63% for t = 18 h; 98% for t = 42 h). When AspA and TarA were hydrogenated using Ru-**b**, the yield of 1,4-BDO was marginal in both cases (~4%), probably due to substrate inhibition of the catalyst. In sharp contrast, the Ir-**a**-derived catalyst is more robust and maintains its activity during the hydrogenation of MliA, AspA, and TarA, to furnish 1,4-BDO in 98%, 66%, and 29% yield, respectively (Fig. 3b, entries 6–8; ESI, Tables S7 and S8; see also proposed multistep HDO/HDA and hydrogenation sequences: ESI, Figs. S3–S5). The formation of 1,4-BDO from MliA and AspA tentatively begins with the dehydrative formation of a five-membered anhydride, followed by (or concurrent with) the β-elimination of H_2O (HDO) or NH_3 (HDA), respectively, to give MleAn, which could then undergo sequential reduction of the olefin and carboxyl groups. The fact that MliA and AspA are convergently and preferentially transformed into their anhydrides was confirmed by several control experiments (ESI, Table S7). In contrast, 1,2-propandiol (1,2-PDO: 36%) is the main product formed from TarA. When NaH (9 mol %) was used for the preactivation of Ir-**a** under otherwise identical conditions, 1,2-PDO and 1,4-BDO were produced in higher (69%) and lower yield (14%), respectively (Fig. 3b, entry 9). Thus, the complex reaction pathway for the formation of 1,2-PDO with 1,4-BDO as a side product may involve the dehydration of TarA to OacA as a common process, followed by two distinct multistep sequences to generate either 1,2-PDO or 1,4-BDO (ESI, Fig. S5). The former involves the facile decarboxylation of the resulting β-ketoacid (OacA,

Fig. 1a) and a subsequent hydrogenation of the remaining keto- and CA parts of 2-oxopropanoic (pyruvic) acid; the latter involves the hydrogenation of the ketone of the β-ketoacid to MliA, followed by the stepwise process described above (MliA→MliAn→MleAn→GBL→1,4-BDO). Indeed, when the potential intermediate OacA, which is the starting compound in the Krebs cycle, was hydrogenated (Ir-**a** (1.5 mol %); NaH (9 mol %); P_{H2} = 6 MPa; T = 180 °C; t = 18 h), 1,2-PDO (38%) was detected, while the formation of 1,4-BDO was negligible (~1%) (Fig. 3b, entry 10; ESI, Tables S9 and S10). The decarboxylation was much faster than the hydrogenation of the ketone. The long-lived catalytic activity of Ir-**a** in the hydrogenation of the three C_4-DCAs is probably due to the almost exhaustive coordinative saturation and steric confinement of the Ir center, which provide structural robustness to the Ir-**a**-derived catalyst. These electronic and steric features prevent substrate/product inhibition of the catalyst, namely, deactivation of the catalyst by the highly functionalized substrates MliA, AspA, and TarA, which are probably able to more tightly ligate the coordinatively less saturated Ru center of Ru-**b** through bidentate chelation.

Reaction of H_2 with C_5- and C_6-PCA. OglA and itaconic acid (ItaA) are C_5-DCAs; the former is a Krebs cycle metabolite (*13, 16*), while the latter can be fermentatively biosynthesized in the cytoplasm through the *cis*-AcoA-decarboxylase-catalyzed decarboxylation of *cis*-AcoA (a C_6 acid involved in the Krebs cycle), which is released from the mitochondria (*32*). Both DCAs undergo hydrogenation using H_2 and Ir-**a**, to furnish 2-($HOCH_2$)-1,4-BDO in 85% yield (isolated yield: >94%) and 2-Me-1,4-BDO in 78% yield, respectively (Fig. 3d, entries 1 and 4). ItaA has previously been hydrogenated to 2-Me-1,4-BDO in 93% yield using a Ru–Triphos catalyst (0.5 mol %) under relatively harsh reaction conditions (T = 195 °C; P_{H2} = 10 MPa; t = 18 h) (*33*). CitA and AcoA are C_6-TCA metabolites in the Krebs cycle (*16*), and their fermentation has previously been investigated (*14, 15*). Although the time required was relatively long (120 h) in both cases, the diol 2-methyl-1,4-BDO was obtained uniformly in 45–47% yield (Fig. 3d, entries 2 and 3). This suggests that the dehydration of CitA gives *cis*- and/or *trans*-AcoA, which is transformed into ItaA upon decarboxylation. The subsequent hydrogenation of ItaA affords 2-Me-1,4-BDO (Fig. 2a).

Reaction of H_2 with miscellaneous DCAs and MCAs. Phthalic acid (PhtA) is a 1,4-DCA formed via the hydration of phthalic anhydride, which is a commodity chemical produced on a large scale in the petrochemical industry. PhtA is an aromatic carboxylic acid, and its CO_2H group is generally more inert to hydrogenation than that of aliphatic carboxylic acids (*8, 33, 34*). In addition, PhtA is difficult to hydrogenate to the corresponding diol, 1,2-bis(1,2-hydroxymethyl)benzene (BHB). Instead, PhtA tends to undergo dearomatic hydrogenation when heterogeneous catalysts are used (*34*). Even using a Ru-Triphos catalyst (1.5 mol %; P_{H2} = 8.5 MPa) (*35*), its ester, dimethyl phthalate, is preferentially hydrogenated to the GBL derivative phthalide (PHT); only under specifically arranged strongly acidic conditions is BHB (78%) the major product (*35*). Neither molecular homogeneous nor heterogeneous catalysts have achieved the selective 8e-reduction/dehydration of the two adjacent CO_2H groups on the benzene ring in more than marginal yield. However, the selective hydrogenation of PhtA to BHB using Ir-**a** was successful when 1,4-dioxane was used instead of toluene as the solvent, giving BHB in 88% yield (11% PHT) (Fig. 3e; ESI, Tables S11–S14). Reducing the reaction temperature from 160 °C to 140 °C under otherwise identical conditions quantitatively furnished PHT (98%), while the reaction in toluene was less efficient (BHB: 44%; PHT: 55%).

Levulinic acid (LevA) is an important C_5-MCA that can be produced artificially from glucose/cellulose with promising scalability (*36*). LevA undergoes hydrogenation using H_2 and Ir-**a** to give 1-Me-1,4-BDO (Fig. 2a) in 94% yield under the standard reaction conditions ($[\text{Ir-}\mathbf{a}]_0$ = 7.5 mM (1.5 mol %); T = 180 °C; t = 18 h; P_{H2} = 6 MPa) (Fig. 3d, entry 5). The reaction tentatively starts with the hydrogenation of the ketone moiety at a much faster reaction rate than that of the hydrogenation of the acid, followed by dehydrative lactonization and finally hydrogenation of the resulting 2- and 3-methyl-γ-butyrolactone (2- and 3-Me-GBL) to 2-Me-1,4-BDO. LevA has previously been hydrogenated to 2-Me-1,4-BDO (95–99%) using a Ru–Triphos catalysts (0.1–2 mol %) under comparable reaction conditions (T = 140–160 °C; P_{H2} = 5–10 MPa; t = 16–18 h) (*8, 33*).

Molecular insights into the behavior of the single-active-site catalyst. Unlike with the deprotonation at the $CH_2P\textit{i}Pr_2$ moiety of Ru-**a**, which is facilitated when NaH is used, Ir-**a** seems to undergo spontaneous tautomerization upon heating in the absence of an alkali base. Indeed, when a CH_3OD/THF-d_8 solution of Ir-**a** was heated to 70 °C for 15 h, the four hydrogen atoms of the two methylene units and the Ir–H were all replaced with deuterium atoms (Fig. 4a; ESI, Figs. S6–S8). Similar H/D exchange was observed during the synthesis of Ir-**a** in CH_3OD at 70 °C from $[\text{Ir(cod)Cl}]_2$ (ESI, Fig. S9). The smooth H–D exchange on the Ir center under mild conditions was tentatively assigned to the hydricity–proticity interchange that occurs in parallel to Ir(III)–Ir(I) interconversion under near-neutral conditions. Similar H–D exchange has also been observed in a D_2O solution of a Cp*IrH(bpy) complex, but only under relatively acidic conditions (pD = 2.4–6.4) (*37*).

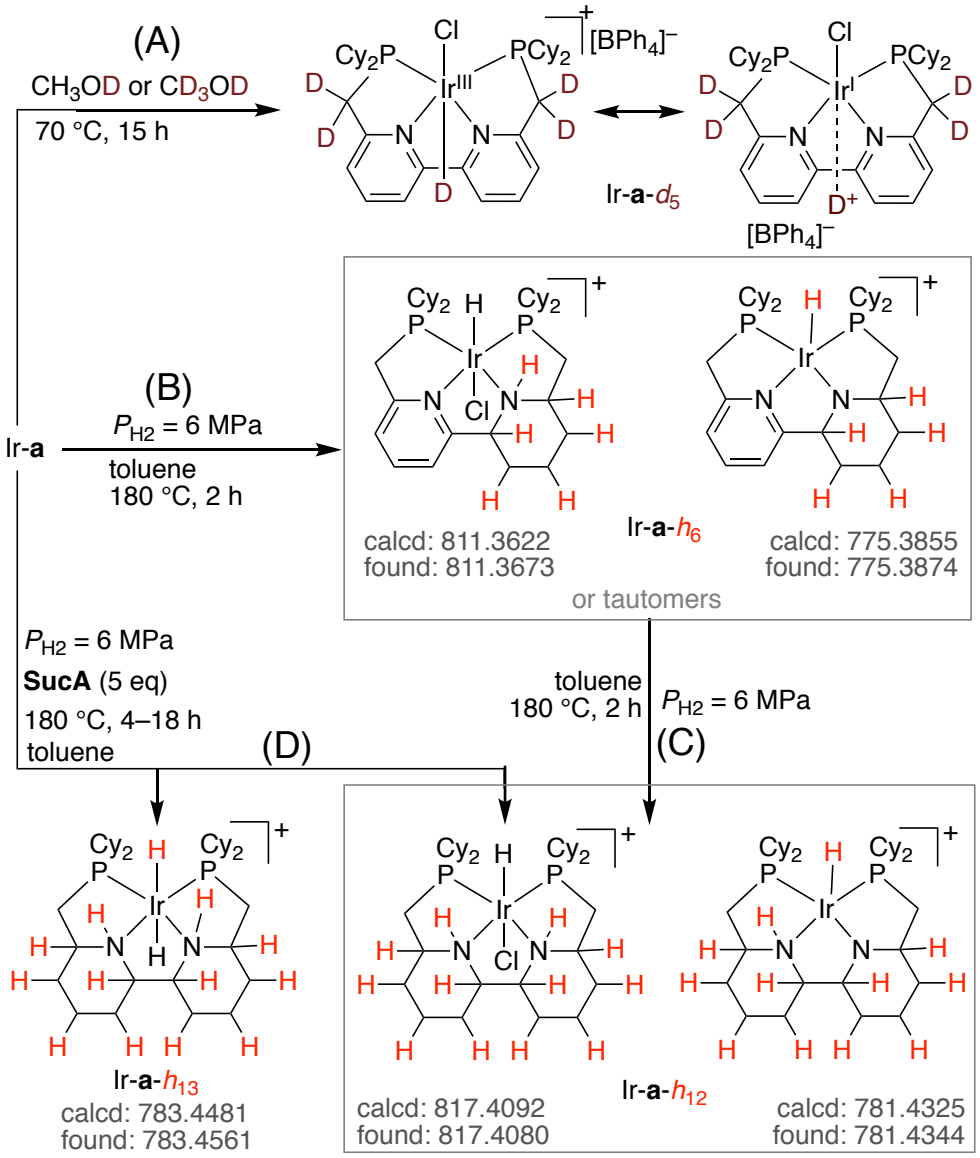

Fig. 4. Representative H/D exchange and structural interconversion of Ir-a under different reaction conditions. (A) Heating in deuterated alcohols without H_2. (B) Shorter heating with H_2. (C) Prolonged heating with H_2. (D) Prolonged heating in the presence of a monocarboxylic acid with H_2. The values below each compound represent theoretical and experimental ESI-MS values.

The facile tautomerization of Ir-**a** under weakly acidic conditions, which could lead to the dearomatization of the dipyridyl fragment, suggests that the hydrogenation of bpy might occur upon heating in the presence of H_2. To verify this hypothesis, in addition to testing the structural robustness of the resting state of the catalyst derived from Ir-**a**, Ir-**a** was activated under the conditions used for the hydrogenation, and the resulting samples were subjected to electron spray ionization-mass spectrometry (ESI-MS) measurements (ESI, Figs. S10–S13). When Ir-**a** was preactivated for 2 h in the absence of SucA (P_{H2} = 6 MPa; T = 180 °C), the mass spectra indicated that Ir-**a**-h_6 was the main intermediate (Fig. 4b), accompanied by the minor species Ir-

a-h_{12} (Fig. 4c). The hydrogenation of bpy was detected, which is consistent with previous results on Ru-**a** (*20*). In contrast, heating the sample for an additional 2 h gave Ir-**a**-h_{12} as the major product. Unlike in the case of Ru-**a**, however, the C–P bonds of Ir-**a** were not cleaved during these processes. When the preactivation of Ir-**a** was carried out in the presence of excess SucA (Ir-**a**:SucA (mol %) = 1:5; $[\mathbf{1a}]_0$ = 7.5 mM; $[\text{SucA}]_0$ = 37.5 mM; in toluene; P_{H2} = 6 MPa; T = 180 °C; t = 4–18 h), SucA was completely consumed, and Ir-**a**-h_{12} (Fig. 4d; ^{1}H NMR (ppm): δ –23.1 (1H, t, J = 16.1 Hz, ClIrH)) and Ir-**a**-h_{13} (Fig. 4d; ^{1}H NMR (ppm): δ –9.29 (2H, t, J = 13.8 Hz, IrH_2)) were the two major products observed, with the C–P bonds acting as spectators. These results suggest that the species that catalyzes the hydrogenation is produced via the incorporation of multiple hydrogen atoms into the precatalyst Ir-**a**. It is highly likely that the Ir center of the catalyst is virtually coordinatively saturated between two apical ligands in *trans* configuration. It could thus be feasibly concluded that two of the hydrogen atoms on the catalytic species "H(δ^-)–Ir–N–H(δ^+)" (*38*) are transferred directly onto olefins and the carbonyl groups of esters, anhydrides, and ketones; however, an alternative proton transfer pathway from the C–H bonds (*29, 39*) of the Ir catalyst cannot be ruled out at this point. To the best of our knowledge, this is the first time that the Noyori-type bifunctional mechanism (*38, 40, 41, 42*) has been experimentally observed in the hydrogenation of carboxylic acid anhydrides.

Inductive argument: Similarities to solid surface catalysis. In many respects, the behavior of the molecular catalyst derived from Ir-**a** resembles that of a catalytic metal (solid) surface on which H_2 is adsorbed: (1) A concomitant hydrogenation and HDO sequence often takes place (*3,43*); this is rarely possible using a single-metal-site catalyst; (2) multiple hydrogen atoms are exposed on the metal surface. These atoms can rapidly exchange with external hydrogen/deuterium atoms to act as both a proton (H^+) and hydride (H^-) source; (3) the solid catalytic surface is composed of a framework of multiple metal- and hetero-atoms. Such surfaces are structurally robust, with their bonding being only slightly (or relatively slowly) damaged even under strenuous reaction conditions; (4) solid surfaces are less susceptible to deactivation or poisoning than molecular catalysts by highly oxygenated and nitrogenated substances; (5) solid hydrogenation catalysts may operate via the conventional but still controversial Eley-Rideal model (*44*), in which a hydrogen atom (or atoms) is transferred via direct interaction of the exposed hydrogen atoms on the solid surface with an organic molecule, i.e., direct chemisorption of the molecule on the surface metal is avoided.

Conclusions. This work demonstrates that a bespoke, structurally robust Ir complex with a tetradentate PNNP ligand can achieve the hydrogenative deoxygenation/deamination of a variety of naturally available bio-renewable C_4–C_6 feedstocks. The conceptually new sterically confined Ir-bpy framework: (1) prefers the uptake of H_2 relative to that of highly functionalized organic compounds; (2) promotes reduction (hydricity) and dehydration (proticity); (3) retains the robust tetracoordinated organic–metal framework under strenuous hydrogenation conditions. This multifunctional, robust, single-active-site molecular catalyst can be used for the hydrogenation of polyacids to polyols as well as for hydrodeoxygenation (HDO) and hydrodeamination (HDA) reactions to give saturated carbon chains under weakly acidic conditions. The structural precatalyst/catalyst platform presented in this work could potentially be extended to develop more versatile catalysis for the hydrogenation and hydrogenolysis of thermodynamically stable and kinetically inert C–O and C–N single bonds as well as other unsaturated bonds; such studies are currently in progress in our laboratory.

References and Notes:

1. T. Werpy, G. Petersen, "Top value added chemicals from biomass volume I–results of screening for potential candidates from sugars and synthesis gas" (U.S. Department of Energy, 2004; http://energy.gov/eere/bioenergy/downloads/top-value-added-chemicals-biomass-volume-i-results-screening-potential).
2. L. Wu, T. Moteki, A. A. Gokhale, D. W. Flaherty, F. D. Toste, Production of fuels and chemicals from biomass: condensation reactions and beyond. *Chem* **1**, 32–58 (2016).
3. A. M. Ruppert, K. Weinberg, R. Palkovits, Hydrogenolysis goes bio: from carbohydrates and sugar alcohols to platform chemicals. *Angew. Chem. Int. Ed.* **51**, 2564–2601 (2012).
4. J. J. Bozell, G. R. Petersen, Technology development for the production of biobased products from biorefinery carbohydrates—the US Department of Energy's "Top 10" revisited. *Green Chem*. **12**, 539–554 (2010).
5. C. Delhomme, D. Weuster-Botz, F. E. Kühn, Succinic acid from renewable resources as a C_4 building-block chemical - A review of the catalytic possibilities in aqueous media. *Green Chem.* **11**, 13–26 (2009).
6. Biotechnology Innovation Organization, "Advancing the biobased economy: Renewable chemical biorefinery commercialization, progress, and market opportunities, 2016 and beyond" (2016; https://www.bio.org/sites/default/files/BIO_Advancing_the_Biobased_Economy_2016.pdf#search=%271%2C4BDO+is+among+the+most+versatile+synthetic+intermediates+and+is+an+important+commodity+chemical+used+to+manufacture+over+2.5+million+tons+annually+of+valuable+polymers+including+poly%28butylene%29+terephthalate+and+poly%28urethane%29s%27).
7. L. Rosi, M. Frediani, P. Frediani, Isotopomeric diols by "one-pot" Ru-catalyzed homogeneous hydrogenation of dicarboxylic acids. *J. Organomet. Chem.* **695**, 1314–1322 (2010).
8. T. vom Stein, M. Meuresch, D. Limper, M. Schmitz, M. Hölscher, J. Coetzee, D. J. Cole-Hamilton, J. Klankermayer, W. Leitner, Highly versatile catalytic hydrogenation of carboxylic and carbonic acid derivatives using a Ru-triphos complex: molecular control over selectivity and substrate scope. *J. Am. Chem. Soc.* **136,** 13217–13225 (2014).
9. S. D. Le, S. Nishimura, Highly selective synthesis of 1,4-butandiol via hydrogenation of succinic acid with supported Cu–Pd alloy nanoparticles. *ACS Sustainable Chem. Eng.* **7**, 18483–18492 (2019).
10. V. Martin-Dominguez, J. Estevez, F. de Borja Ojembarrena, V. E. Santos, M. Ladero, Fumaric acid production: a biorefinery perspective. *Fermentation* **4**, 33 (2018).
11. T. P. West, Microbial production of malic acid from biofuel-related coproducts and biomass. *Fermentation* **3**, 14 (2017).
12. G. A. Abdel-Tawab, E. Broda, G. Kellner, The production of pyruvic acid, oxaloacetic acid and α-oxoglutaric acid from glucose by tissue in culture. *Biochem. J*. **72**, 619–623 (1959).

13. B. Beer, A. Pick, V. Sieber, In vitro metabolic engineering for the production of α-ketoglutarate. *Metab. Eng.* **40**, 5–13 (2017).

14. K. Kobayashi, J. Maruebi, K. Kirimura, Bioproduction of *trans*-aconitic acid from citric acid by whole-cell reaction of *Escherichia coli* heterologously expressing the aconitate isomerase gene from *Pseudomonas* sp. WU-0701. *ChemistrySelect* **1**, 1467–1471 (2016).

15. P. L. Show, K. O. Oladele, Q. Y. Siew, F. A. A. Zakry, J. C.-W. Lan, T. C. Ling, Overview of citric acid production from *Aspergillus niger*. *Front. Life Sci.* **8**, 271–283 (2015).

16. H. A. Krebs, W. A. Johnson, Metabolism of ketonic acids in animal tissues. *Biochem. J.* 31, 645–660 (1937).

17. T. J. Korstanje, R. J. M. Klein Gebbink, Catalytic oxidation and deoxygenation of renewables with rhenium complexes. *Top. Organomet. Chem*. **39**, 129–174 (2012).

18. E. Furimsky, Catalytic hydrodeoxygenation. *Applied Catalysis A: General* **199**, 147–190 (2000).

19. J. Pritchard, G. A. Filonenko, R. van Putten, E. J. M. Hensen, E. A. Pidko, Heterogeneous and homogeneous catalysis for the hydrogenation of carboxylic acid derivatives: History, advances and future directions. *Chem. Soc. Rev.* **44**, 3808–3833 (2015).

20. T. Miura, M. Naruto, K. Toda, T. Shimomura, S. Saito, Multifaceted catalytic hydrogenation of amides via diverse activation of a sterically confined bipyridine–ruthenium framework. *Sci. Rep.* **7**, 1586 (2017).

21. T. Miura, I. E. Held, S. Oishi, M. Naruto, S. Saito, Catalytic hydrogenation of unactivated amides enabled by hydrogenation of catalyst precursor. *Tetrahedron Lett*. **54**, 2674–2678 (2013).

22. S. Yoshioka, S. Saito, Catalytic hydrogenation of carboxylic acids using low-valent and high-valent metal complexes. *Chem. Commun*. **54**, 13319–13330 (2018).

23. M. Naruto, S. Agrawal, K. Toda, S. Saito, Catalytic transformation of functionalized carboxylic acids using multifunctional rhenium complexes. *Sci. Rep.* **7**, 3425 (2017).

24. M. Naruto, S. Saito, Cationic mononuclear ruthenium carboxylates as catalyst prototypes for self-induced hydrogenation of carboxylic acids. *Nat. Commun.* **6**, 8140 (2015).

25. A. Saito, S. Yoshioka, M. Naruto, S. Saito, Catalytic hydrogenation of *N*-protected α-amino acids using ruthenium complexes with monodentate phosphine ligands. *Adv. Synth. Catal.* **362**, 424–429 (2020).

26. Y. Takada, J. Caner, H. Naka, S. Saito, Photocatalytic transfer hydrogenolysis of allylic alcohols for rapid access to platform chemicals and fine chemicals. *Pure Appl. Chem.* **90**, 167–174 (2018).

27. R. Crabtree, Iridium compounds in catalysis. *Acc. Chem. Res*. **12**, 331–337 (1979).

28. J. Zhang, G. Leitus, Y. Ben-David, D. Milstein, Efficient homogeneous catalytic hydrogenation of esters to alcohols. *Angew. Chem. Int. Ed*. **45**, 1113–1115 (2006).

29. C. Gunanathan, D. Milstein, Metal ligand cooperation by aromatization-dearomatization: a new paradigm in bond activation and "green" catalysis. *Acc. Chem. Res*. **44**, 588–602 (2011).

30. G.N. Cohen, “The aspartic acid family of amino acids. Biosynthesis” in *Microbial Biochemistry* (Springer, Dordrecht, 2004), pp. 139–149.

31. S. DeBolt, D. R. Cook, C. M. Ford, L-Tartaric acid synthesis from vitamin C in higher plants. *Proc. Natl. Acad. Sci. U.S.A.* **103**, 5608–5613 (2006).

32. M. Zhao, X. Lu, H. Zong, J. Li, B. Zhuge, Itaconic acid production in microorganisms. *Biotechnol. Lett.* **40**, 455–464 (2018).

33. F. M. A. Geilen, B. Engendahl, A. Harwardt, W. Marquardt, J. Klankermayer, W. Leitner, Selective and flexible transformation of biomass-derived platform chemicals by a multifunctional catalytic system. *Angew. Chem. Int. Ed*. **49**, 5510–5514 (2010).

34. M. Tang, S. Mao, X. Li, C. Chen, M. Li, Y. Wang, Highly effective Ir-based catalysts for benzoic acid hydrogenation: experiment- and theory-guided catalyst rational design. *Green Chem.* **19**, 1766–1774 (2017).

35. H. T. Teunissen, Homogeneous ruthenium catalyzed hydrogenation of esters to alcohols. *Chem. Commun*. 1367–1368 (1998).

36. K. Yan, C. Jarvis, J. Gu, Y. Yan, Production and catalytic transformation of levulinic acid: a platform for specialty chemicals and fuels. *Renew. Sustain. Energy Rev.* **51**, 986–997 (2015).

37. T. Abura, S. Ogo, Y. Watanabe, S. Fukuzumi, Isolation and crystal structure of a water-soluble iridium hydride: a robust and highly active catalyst for acid-catalyzed transfer hydrogenations of carbonyl compounds in acidic media. *J. Am. Chem. Soc.* **125**, 4149–4154 (2003).

38. T. J. Schmeier, G. E. Dobereiner, R. H. Crabtree, N. Hazari, Secondary coordination sphere interactions facilitate the insertion step in an iridium(III) CO_2 reduction catalyst. *J. Am. Chem. Soc.* **133**, 9274–9277 (2011).

39. H. Li, X. Wang, F. Huang, G. Liu, J. Jiang, Z.-X. Wang, Computational study on the catalytic role of pincer ruthenium(II)-PNN complex in directly synthesizing amide from alcohol and amine: the origin of selectivity of amide over ester and imine. *Organometallics* **30**, 5233–5247 (2011).

40. C. A. Sandoval, T. Ohkuma, K. Muñiz, R. Noyori, Mechanism of asymmetric hydrogenation of ketones catalyzed by BINAP/1,2-diamine-ruthenium(II) complexes, *J. Am. Chem. Soc.* **125**, 13490–13503 (2003).

41. L. V. A. Hale, N. K. Szymczak, Hydrogen transfer catalysis beyond the primary coordination sphere. *ACS Catal.* **8**, 6446–6461 (2018).

42. R. Tanaka, M. Yamashita, K. Nozaki, Catalytic hydrogenation of carbon dioxide using Ir(III)-pincer complexes. *J. Am. Chem. Soc*. **131**, 14168–14169 (2009).

43. H. Kobayashi, H. Ohta, A. Fukuoka, Conversion of lignocellulose into renewable chemicals by heterogeneous catalysis. *Catal. Sci. Technol.* **2**, 869–883 (2012).

44. B. Jackson, X. Sha, Z. B. Guvenc, Kinetic model for Eley-Rideal and hot atom reactions between H atoms on metal surfaces. *J. Chem. Phys.* **116**, 2599–2608 (2002).

Acknowledgments: We acknowledge Mrs. K. Oyama, Y. Maeda, H. Okamoto, and Ms. H. Natsume for technical support.
Funding: This work was supported by a Grant-in-aid for Scientific Research on Innovative Area (18H04247, to SS) from MEXT, and partially by the Asahi Glass Foundation (Step-up-grant, to SS) and by Scientific Research (B) (19H02713, to SS) from JSPS.
Author contributions: SN first synthesized the Ir complexes and discovered and developed the hydrogenation of C_4-DCAs. SY (who completed the research) and MN contributed equally to the other experimental work. SS organized the overall research and wrote the manuscript.
Competing interests: Authors declare no competing interests.
Data and materials availability: All data is available in the main text or the supplementary materials.

Supplementary Materials: